TISSUE ENGINEERING: Part B
Volume 19, Number 3, 2013

DOI: 10.1089/ten.teb.2012.0340

Comparison of Methods for Whole-Organ Decellularization in Tissue Engineering of Bioartificial Organs

Ming He, MBBS,[1] and Anthony Callanan, Ph.D.[1,2]

Organ transplantation is now a well-established procedure for the treatment of end-stage organ failure due to various causes, but is a victim of its own success in that there is a growing disparity in numbers between the donor organ pool available for transplantation and the patients eligible for such a procedure; hence, an alternative solution to the limited donor organ pool is both desirable and necessary. Tissue engineering is an interdisciplinary field that applies the principles of engineering and life sciences toward the development of functional replacement tissues for clinical use. A recent innovation in tissue and organ engineering is the technique of whole-organ decellularization, which allows the production of complex three-dimensional extracellular matrix (ECM) bioscaffolds of the entire organ with preservation of the intrinsic vascular network. These bioscaffolds can then be recellularized to create potentially functional organ constructs as a regenerative medicine strategy for organ replacement. We review the current applications and methods in using xenogeneic whole-organ ECM scaffolds to create potentially functional bioartificial organ constructs for surgical implantation, and present a comparison of specific trends within this new and developing technique.

Introduction

Organ transplantation is now a well-established procedure for the treatment of end-stage organ failure due to various causes, but is a victim of its own success in that there is a growing disparity in numbers between the donor organ pool available for transplantation and the patients eligible for such a procedure, with a high mortality rate in those who are on the waiting list. While there is ongoing debate to address this issue with strategies, both within a wider social or legislative context (e.g., so-called opt-out or presumed consent organ donation[1]) and others more specifically applicable to certain groups (e.g., living kidney donation), these strategies can be either controversial or not without additional clinical risk (e.g., to the living donor). An alternative solution to the limited donor organ pool is both desirable and necessary.

Tissue engineering is an interdisciplinary field that applies the principles of engineering and life sciences toward the development of functional replacement tissues for clinical use. Many developments within this field employ the seeding and cultivation of cells onto acellular scaffolds; however, control and utilization of the types of cell, scaffold material, interactions between the two, and the optimal conditions for the regeneration of functional tissue replacement are complex and vary from the nano- to macroscale.[2] One group of biological scaffold materials that are already commonly in use for a variety of reconstructive surgical applications is that derived from the extracellular matrix (ECM).[3] The ECM is secreted by the resident cells of each tissue and organ, and scaffolds derived from this material are produced by the process of decellularization of the specific tissue.[4]

A recent innovation in decellularization is the generation of whole-organ ECM scaffolds.[5–9] This is a new technique in the application of decellularization agents (e.g., detergents) by using antegrade or retrograde perfusion of the inherent vascular network within the organ. This technique has led to the production of so-called bioartificial scaffolds[10,11] that preserve the three-dimensional (3D) ECM structure of an organ in its entirety.[10–27] This complete 3D structure gives site-specific architecture and composition, which control function at a local level within the organ. This scaffold can then be subsequently repopulated with cells using the same perfusion technique to produce organ regeneration to a functional degree. This type of scaffold combines the natural advantages and properties of the ECM in promoting and regulating cell proliferation and differentiation, the organizational and architectural complexity of the whole organ, as well as the supportive vascular network for the provision of oxygen and nutrients required for 3D tissue metabolism. This work has been carried out with preliminary success in animal studies of the heart,[10] the lungs,[11,14,21] and the liver,[17] and the decellularized whole-organ scaffold has also been

[1]Department of Bioengineering and Materials, Institute of Biomedical Engineering, Imperial College London, London, United Kingdom.
[2]Centre for Applied Biomedical Engineering Research (CABER), Department of Mechanical, Aeronautical and Biomedical Engineering, and Materials and Surface Science Institute, University of Limerick, Ireland.

produced in the kidney,[18–20] as well other tissues such as small bowel[26] and skeletal muscle.[27]

We review the current applications and methods in using xenogeneic whole-organ ECM scaffolds to create potentially functional bioartificial organ constructs for surgical implantation, and compare specific trends within this new and developing technique to give a concise overview of existing experimental work across all the relevant organ systems as a tool for researchers.

The ECM

The ECM is the naturally occurring scaffold material secreted and manufactured by the resident cells of each tissue and organ. The complex 3D organization of the ECM and its components are dictated by the tissue from which the ECM is derived and can be considered specific to that tissue or organ[28–30]; however, individual components are common throughout most tissues such as collagen, laminin, fibronectin, and hyaluronic acid. The structural and functional molecules of the ECM are in a state of dynamic equilibrium within the surrounding microenvironment,[31] and also provide the means by which cells communicate with each other and the external environment.[32,33] By definition, the ECM possesses the ideal characteristics of the tissue-engineered scaffold or biomaterial (in addition to the functions already described), being biocompatible, a supportive medium for blood vessels, nerves, and lymphatics and for the diffusion of nutrients from the blood, as well as being able to undergo constructive remodeling and degradation within the body's own systems.[34–36]

The Properties of ECM

Bioinductive properties of ECM

The ability of the ECM scaffold to facilitate and integrate cellular and external environmental cues is the consequence of its bioinductive properties, allowing the constructive remodeling of tissue after the *in vivo* implantation of ECM scaffolds.[37–39] This remodeling cannot be solely attributed to characteristics such as viscoelastic behavior, biomechanical properties, or host cell attachment through collagen, fibronectin, and laminin ligands within the ECM. Growth factors such as vascular endothelial growth factor,[40] basic fibroblast growth factor,[41,42] and transforming growth factor-beta[44,45] are responsible for crucial events of remodeling such as angiogenesis, abundant host cell infiltration, mitogenesis, and deposition and organization of new host ECM. These can survive tissue processing and terminal sterilization[41,43,44] to exert an effect on tissue remodeling and are released during the degradation of the ECM scaffold.[40–45] Indeed, the degradation process itself, which is mediated by enzymatic and cellular processes, may be considered as a mechanism for controlled release of the ECM constituent molecules. The process of degradation and growth factor release continues until the scaffold is completely degraded. Degradation products of the molecules that constituted the ECM may mediate a subsequent series of remodeling events. These subsequent events include the release of cryptic peptides that initiate and sustain the recruitment of circulating, bone marrow-derived undifferentiated progenitor cells that actively participate in long-term tissue remodeling,[46,47] the generation of antimicrobial peptides that protect the remodeling site from pathogens,[48–53] other peptides that modulate angiogenesis, and the recruitment of endothelial cells over periods up to 6–8 weeks.[54]

Biomechanical properties of ECM

The mechanical properties of the ECM can be predominantly understood from the combination of its collagen fiber architecture and kinematics. The tissue from which an ECM scaffold is harvested will define its structural characteristics (such as fiber size, orientation, and alignment) and mechanical properties. For instance, small intestinal submucosa (SIS)-derived ECM has been shown to have a preferred fiber alignment in a spiral arrangement along the longitudinal axis of the small intestine,[40,55,56] and it is likely that this structural arrangement facilitates dilation and retraction of the small intestine during peristalsis and transport of intraluminal contents. An understanding of the collagen fiber structure from each organ is important to closely match the scaffold mechanical properties to those of the intended target organ.

Degradation and constructive remodeling of ECM

The bioinductive properties of ECM scaffolds depend crucially on the efficient and effective degradation of the scaffold material and facilitate the constructive remodeling of injured tissue. The species of origin, tissue of origin, and processing techniques during the production of the ECM scaffold can differ markedly and factors such as method of decellularization, use of chemical crosslinking agents, and means of sterilization can affect the degradability and host response to the scaffold material.[57] Quantitative studies of ^{14}C-labeled SIS used in augmentation cystoplasty[58] and Achilles tendon reconstruction[59] procedures have shown that 50% or more of the ECM scaffold is degraded and removed from the implantation site by 28 days. The degradation products are excreted via the urine with no recycling to other tissues. Furthermore, the replacement of the degraded SIS with functional (and similar to normal) host tissue occurred without the loss-of-function, for example, bladder or tendon rupture suggests a rapid infiltration and/or proliferation of functional host cells at the remodeling site with deposition of new ECM. In these two models of degradation analysis, there was also the critical involvement of biomechanical factors such as physiological bladder filling and emptying[38] or progressive weight bearing postoperatively in the tendon repair model.[34] Environmental factors may also play an important role in determining *in situ* regeneration or transformation of implanted tissues, such as that seen in the formation of host-derived tracheal tissue within a long segment of allogenic aortic graft transplanted as a potential conduit for tracheal replacement.[60,61] Hence, understanding of the additional factors that modulate remodeling is also essential to utilize ECM scaffolds effectively.

Host immune response to xenogeneic ECM

Most ECM scaffold biomaterials and commercially available surgical implants are of xenogeneic origin, such as a porcine or bovine source with a few types from human allogeneic tissue.[3] Nonhuman biomaterials have been used in humans for many years without evidence of adverse

host immunological outcomes, for example, porcine heart valve replacements and porcine and bovine insulin for the treatment of diabetes mellitus. Xeno- and allogeneic cellular antigens (e.g., cell membrane Gal epitope) are by definition recognized as foreign by the host and can induce a hyperacute rejection response after organ xenotranplantation; however, components of the ECM are generally conserved among species and tolerated well. With the SIS ECM, complement activation or cell-mediated rejection response does not occur even with the small amounts of Gal epitope that are present,[62,63] and this could be further prevented with either use of transgenic gal knockout animals for tissue harvesting or treatment of harvested ECM with galactosidase.

In terms of the cell-mediated immune response, the Th1 lymphocyte phenotype is associated with macrophage activation, complement fixation, and CD8+ cytotoxic cell differentiation, and activation of the Th1 pathway is implicated in transplant rejection.[64,65] In contrast, activation of the Th2 lymphocyte pathway does not lead to these events, differs markedly both in the profile of cytokines and antibody isotypes produced, and is hence associated with transplant acceptance.[66,67] Implantation studies of the SIS ECM in mice have shown that a Th2 type immune response occurs, similar to that elicited by syngeneic muscle tissue.[68,69]

The likely innate immune-mediated inflammatory response to ECM materials and bioscaffolds also plays an important role in their degradation *in situ* and subsequent constructive remodeling process, and this can be demonstrated by the macrophage phenotype response. Macrophages are phenotypically and functionally plastic, but can be broadly characterized into a polarized M1/M2 phenotype classification, which forms a parallel to the Th1/Th2 response in that M1 macrophages are associated with a proinflammatory and M2 with a constructive remodeling response.[70] The constructive remodeling process can be correlated with the ability of the implanted material to direct the macrophage phenotype, and the ECM has been shown to promote the switch from M1 to M2 after implantation.[71,72] However, the use of chemical crosslinking agents that may interfere with the macrophage-mediated breakdown of the ECM material inhibits the beneficial M2 phenotype and leads to chronic inflammation and fibrosis.[73]

Hence, it can be seen that the overall host immune response for any particular ECM material will be variable and dependent on the diversity of tissue sources and processing methods used in its preparation.

Decellularization and Processing of ECM Scaffolds

Because of the complexity of the 3D organization and composition of all the structural and functional molecules of the ECM that have not yet been fully characterized (and for each type of tissue), it is not currently possible to synthesize this biomaterial in the laboratory. Hence, ECM scaffolds are produced by the process of decellularization of naturally derived tissues, and this can be achieved by a variety of agents and techniques.[3] The complexity and length of the decellularization protocol are correlated with the degree of structural and biological conservation required for the postprocessed tissue, especially for composite tissues and whole organs. Any agent or method will cause some disruption of the ECM composition and ultrastructure, and minimization of these effects is desirable as complete avoidance is not yet feasible. While it is not possible to remove 100% of cellular material from the ECM, it is possible to quantitatively assay cell components such as DNA, mitochondria, and membrane phospholipids. Residual cellular and nuclear material may contribute to cytocompatibility problems *in vitro* and adverse host responses *in vivo*.[74–77] It is also necessary to sterilize ECM scaffolds before *in vitro* use or implantation, as well as the removal of pyrogens (such as endotoxins and intact viral and bacterial DNA) that may be present.

Biological scaffolds may be sterilized by simple treatments such as incubation with acids or solvents, or other treatments such as ethylene oxide exposure, gamma-radiation, and electron beam irradiation. While the simple methods can lack penetration or may damage key ECM components,[78] the latter ones can affect ECM ultrastructure and mechanical properties,[79–81] and newer methods such as supercritical carbon dioxide requires further investigation.[82] Hence, this necessary process is another factor that can critically influence the properties of the bioscaffold, and must be taken into account during the wider-scale standardization and quality assurance of such ECM products before clinical translation.

Whole-Organ Decellularization: Perfusion–Decellularization

This is a relatively new technique that uses anterograde or retrograde perfusion via the intrinsic vascular network as a means of applying the decellularizing agent while largely preserving the 3D architecture of the organ from which the ECM has been isolated. It is the only technique to allow decellularization of thick 3D tissue sections or complete organs in a way that was not previously possible. Since the vascular network exists to minimize the diffusion distance for oxygen to cells, this is a particularly efficient way of delivering decellularizing agents throughout the tissue and transporting the cellular material from the tissue. The vascular network remains intact even after full decellularization has been achieved, hence offering a route for the efficient delivery and penetration of cells and nutrients into the ECM scaffold during the process of recellularization to create a functional organ construct (see Fig. 1 for the schematic diagram of the life cycle of whole-organ decellularization and potential clinical applications).

An Overview of Whole-Organ Decellularization Work

The heart

The first report in which whole-organ decellularization was successfully performed was on the heart.[10] The aorta of a rat heart was cannulated to allow retrograde coronary perfusion with heparinized phosphate-buffered saline with adenosine, 1% sodium dodecyl sulfate (SDS), and 1% Triton X-100 in sequence alternating with rinsing with deionized water between steps. This produced a decellularized scaffold that was structurally similar to the heart, but had a translucent white appearance throughout (Fig. 2). Reimplantation of the acellular heart scaffold onto the aorta demonstrated an intact and patent vascular network (Fig. 3). Recellularization of the heart scaffold with cardiomyocytes under electrophysiological stimulation formed a construct capable of muscular contraction.

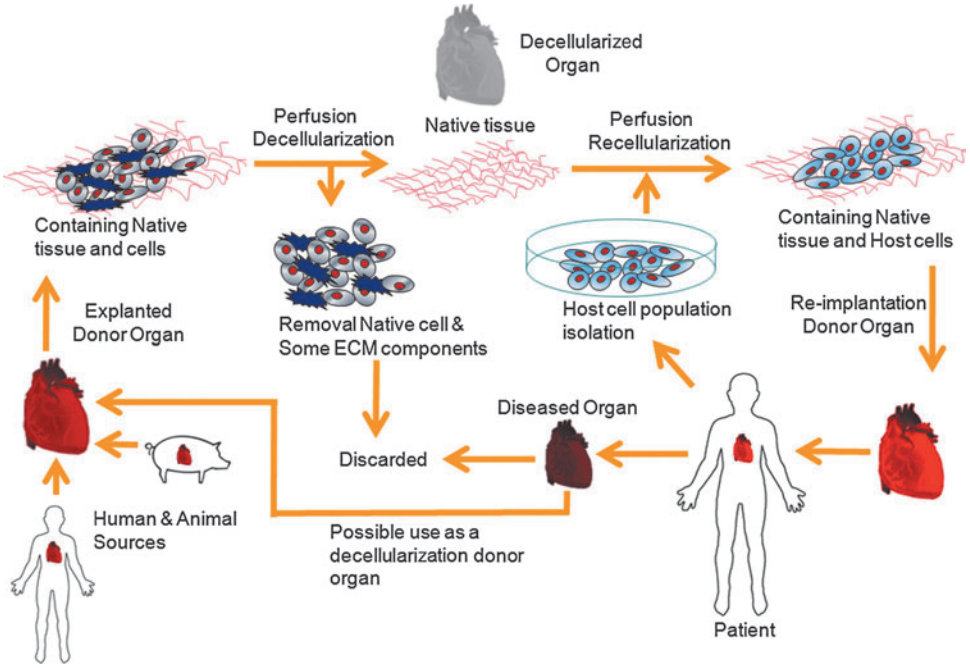

FIG. 1. Schematic diagram of the life cycle of whole-organ decellularization and potential clinical applications. Color images available online at www.liebertpub.com/teb

The lungs

A number of groups have investigated the use of perfusion decellularization in the lungs,[11,13–15,21] which contain two accessible compartments separated by a short diffusion distance, that is, the vascular and the airway systems, by using varying protocols of vascular perfusion alone,[11,21] or in combination with endotracheal instillation,[14,15] or perfusion of the airway compartment.[13] The decellularizing agents used were also far more varied from protocol to protocol, from SDS at different concentrations[11,13,21] to 8 mM CHAPS,[14] to a combination of Triton X-100/deoxycholate/DNAse/bleach.[15] All groups demonstrated preservation of the major components of the ECM and the micro- and macroarchitecture of the lung. Recellularization was achieved with all the reports, although Petersen *et al.* mimicked physiological conditions within the bioreactor by ventilation of the airway compartment at negative pressure at 1 breath/min, and maintained pulmonary artery pressure at 20 mmHg or below. Orthotopic implantation of these tissue-engineered lung constructs demonstrated active gas exchange occurring via sampling of pulmonary arterial and venous blood. However, results in this study and Ott *et al.* showed vascular leakage and pulmonary edema after a few hours of implantation, indicating damage to the microvasculature from the decellularization process. In a follow-up study to Ott *et al.*, Song *et al.* demonstrated further optimization of graft preservation and oxygenative function post-implantation for as long as 7 days.[21] Recellularization was performed with mixtures of whole-lung cell isolates in four cases,[11,14,15,21] but one group used a homogeneous mouse embryonic stem cell population,[13] which showed that the matrix was capable of promoting site-appropriate differentiation without any other specific differentiation cues.

The liver

Liver decellularization has been performed by antegrade perfusion via the portal vein with SDS and Triton X-100, either alone or in combination,[16,17,23,24] although another study used trypsin/EGTA,[25] and Baptista *et al.* used Triton X-100 in combination with ammonium hydroxide.[18,22] Decellularization was demonstrated with histology and evidence of DNA removal, and retention of key ECM constituents with preservation of microvasculature and ECM

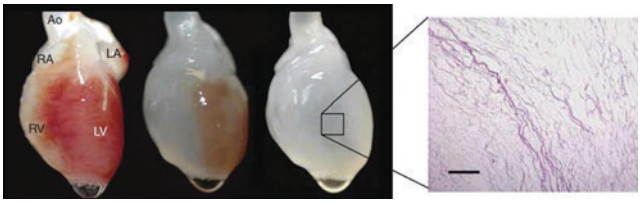

FIG. 2. The heart in stages of increasing decellularization over time with 1% sodium dodecyl sulfate as the decellularizing agent, with the end result of a translucent appearing heart-like scaffold structure. The panel on the right shows histological evidence (H&E staining) of decellularization. Reproduced from [8]. Scale bar = 200 μm. Color images available online at www.liebertpub.com/teb

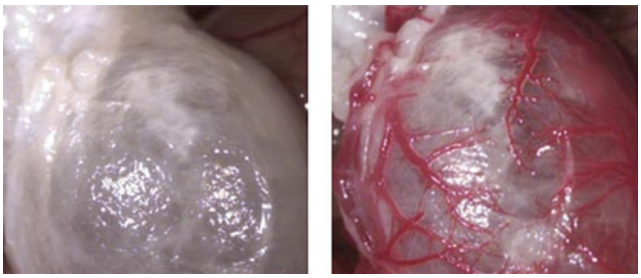

FIG. 3. Coronary perfusion and evidence of intact coronary vasculature (right) after orthotopic implantation of the decellularized heart scaffold (left) and unclamping of the aorta. Reproduced from [8]. Color images available online at www.liebertpub.com/teb

Table 1a. Summary of Species and Strain Used for Decellularization

Organ	*Authors*	*Species (strain)*
Heart	Ott *et al.*, 2008	Rat (Fischer 344)
Heart	Wainwright *et al.*, 2010	Pig
Lung	Ott *et al.*, 2010	Rat (Sprague Dawley)
Lung	Petersen *et al.*, 2010	Rat (Fischer 344)
Lung	Cortiella *et al.*, 2010	Rat
Lung	Price *et al.*, 2010	Mouse (C57BL/6)
Lung	Song *et al.*, 2011	Rat (Sprague-Dawley)
Liver	Uygun *et al.*, 2010	Rat (Lewis)
Liver	Shupe *et al.*, 2010	Rat (Fischer 344)
Liver	Soto-Gutierrez *et al.*, 2011	Rat (Sprague-Dawley)
Liver	Baptista *et al.*, 2011	Ferret
Liver	De Kock *et al.*, 2011	Rat (Sprague-Dawley)
Liver	Barakat *et al.*, 2011	Pig (Yorkshire)
Kidney	Ross *et al.*, 2009	Rat (Sprague-Dawley)
Kidney	Liu *et al.*, 2009	Rat (Wistar)
Liver, Kidney, Pancreas, Small bowel	Baptista *et al.*, 2009	Ferret liver Pig kidney/pancreas/small bowel
Small bowel	Totonelli *et al.*, 2012	Rat (Sprague-Dawley)
Skeletal muscle	Perniconi *et al.*, 2012	Mouse (BALB/C)

Table 1b. Summary of Decellularization Agents Used

Organ	*Authors*	*SDS*	*SDS + Triton*	*Other*
Heart	Ott *et al.*, 2008	(+)	+	−
Heart	Wainwright *et al.*, 2010	−	−	+
Lung	Ott *et al.*, 2010	(+)	+	−
Lung	Petersen *et al.*, 2010	−	−	+
Lung	Cortiella *et al.*, 2010	+	−	−
Lung	Price *et al.*, 2010	−	−	+
Lung	Song *et al.*, 2011	(+)	+	−
Liver	Uygun *et al.*, 2010	(+)	+	−
Liver	Shupe *et al.*, 2010	(+)	+	−
Liver	Soto-Gutierrez *et al.*, 2011	−	−	+
Liver	Baptista *et al.*, 2011	−	−	+
Liver	De Kock *et al.*, 2011	(+)	+	−
Liver	Barakat *et al.*, 2011	+	−	−
Kidney	Ross *et al.*, 2009	(+)	+	−
Kidney	Liu *et al.*, 2009	(+)	+	−
Liver, Kidney, Pancreas, Small bowel	Baptista *et al.*, 2009	−	−	+
Small bowel	Totonelli *et al.*, 2012	−	−	+
Skeletal muscle	Perniconi *et al.*, 2012	+	−	−

SDS, sodium dodecyl sulfate.

ultrastructure. Hepatocytes were seeded onto the acellular liver scaffold via portal vein perfusion and were shown to be functional in four studies[17,22,24,25] by showing evidence of synthesis of lactate dehydrogenase, albumin, and urea after heterotopic implantation. In particular, two studies attempt to scale-up this approach to further approximate human-scale engineered organ constructs by use of ferret[22] and porcine[24] livers, and both studies seeded the bioscaffolds with human liver cells, which were shown to be compatible on these xenogeneic scaffolds.

The kidney

Several groups have decellularized whole kidneys by the perfusion method with preservation of the vascular network and complete cell removal.[18–20] Decellularizing agents vary from 1% Triton or SDS[18,19] to 3% Triton with DNase and additional 4% SDS.[20] The preservation and presence of ECM constituents such as laminin and collagen IV were also demonstrated, as well as collagen I, fibronectin, and heparin sulfate in a separate study, which did not employ perfusion.[83] The latter study juxtaposed fetal cells in fresh renal explants with the ECM scaffolds by layering fetal kidney tissue against the ECM, which supported developmental renal phenotypes in these cells after they migrated into the ECM. In the study by Ross *et al.*, decellularized rat kidneys scaffolds were reseeded with murine embryonic stem cells, and the renal ECM was shown to support the renal differentiation of the embryonic stem cells.

Other tissues/organs

The technique of whole-organ decellularization is also expanding into other tissues and organs such as the small

Table 1c. Summary of Conditions Used for Perfusion Decellularization

Organ	*Authors*	*Flow rate*	*Perfusion pressure*	*Duration of decellularization (perfusion)*
Heart	Ott *et al.*, 2008	-	77.5 mm Hg	12–13 h
Heart	Wainwright *et al.*, 2010	1.3L/min	-	6–7 h
Lung	Ott *et al.*, 2010	-	30 mm Hg	2–3 h
Lung	Petersen *et al.*, 2010	-	< 20 mm Hg	(Total 500 mL perfused)
Lung	Cortiella *et al.*, 2010	N/A	N/A	N/A
Lung	Price *et al.*, 2010	N/A	N/A	N/A
Lung	Song *et al.*, 2011	-	80 cm H_2O	2–3 h
Liver	Uygun *et al.*, 2010	1 mL/min	-	5 days
Liver	Shupe *et al.*, 2010	5 mL/min	-	(Total 300 mL × 4 perfused)
Liver	Soto-Gutierrez *et al.*, 2011	8 mL/min	-	20–26 h
Liver	Baptista *et al.*, 2011	5 mL/min	-	(Total 40 × + 50 × volume of the liver)
Liver	De Kock *et al.*, 2011	30 mL/min	-	1–2 h
Liver	Barakat *et al.*, 2011	-	80 mm Hg	2–3 days
Kidney	Ross *et al.*, 2009	-	100 mm Hg	(Not stated)
Kidney	Liu *et al.*, 2009	-	100 cm H_2O	12–13 h
Liver, Kidney, Pancreas, Small bowel	Baptista *et al.*, 2009	10–60 mL/min	-	24 h
Small bowel	Totonelli *et al.*, 2012	0.6 mL/h	-	31 h (per DET cycle)
Skeletal muscle	Perniconi *et al.*, 2012	N/A	N/A	24–48 h

Table 1d. Summary of Decellularized Whole-Organ Scaffold Characterization and Techniques

Organ	*Authors*	*Histology/ IHC*	*EM*	*Quantitative assay for DNA/ECM components*	*Vascular characterization*	*Mechanical testing*
Heart	Ott *et al.*, 2008	+ / +	+	-	Corrosion casting + implantation	+
Heart	Wainwright *et al.*, 2010	+ / +	+	+	-	+
Lung	Ott *et al.*, 2010	+ / –	+	-	-	+
Lung	Petersen *et al.*, 2010	+ / +	+	-	Micro-CT	+
Lung	Cortiella *et al.*, 2010	– / – (IF)	-	(Gel electrophoresis for DNA)	-	-
Lung	Song *et al.*, 2011	-	-	-	-	-
Lung	Price *et al.*, 2010	+ / +	+	+	-	+
Liver	Uygun *et al.*, 2010	+ / +	+	+	Corrosion casting	-
Liver	Shupe *et al.*, 2010	+ / +	-	-	-	
Liver	Soto-Gutierrez *et al.*, 2011	+ / +	+	(Gel electrophoresis for DNA)	Corrosion casting	-
Liver	Baptista *et al.*, 2011	+ / +	+	+	Fluoroscopy + confocal microscopy	-
Liver	De Kock *et al.*, 2011	+ / +	+	-	Corrosion casting	-
Liver	Barakat *et al.*, 2011	+ / +	-	-	Corrosion casting + fluoroscopy	
Kidney	Ross *et al.*, 2009	+ / +	+	-	-	-
Kidney	Liu *et al.*, 2009	+ / – (IF)	+	-	-	-
Liver, Kidney, Pancreas, Small bowel	Baptista *et al.*, 2009	+ / –	-	-	Fluoroscopy	-
Small bowel	Totonelli *et al.*, 2012	+ / +	+	+	-	+
Skeletal muscle	Perniconi *et al.*, 2012	+ / +	-	-	-	-

IHC, immunohistochemistry; EM, electron microscopy; IF, immunofluorescence; ECM, extracellular matrix.

bowel and skeletal muscle, especially as it has the potential to allow the development of a viable replacement in the absence of any current clinical alternative, for example, intestinal failure and large-muscle defects due to trauma. Totonelli *et al.* have demonstrated the application of this technique to small bowel[26] and shown the viability of amniotic fetal stem cells seeded onto the decellularized scaffold and its angiogenic properties, although perfusion recellularization was not performed. Perniconi *et al.* have decellularized whole skeletal muscles derived from rats by an incubation method, and further have implanted the acellular scaffolds *in vivo* within an equivalent muscle defect to show infiltration of inflammatory and stem cells within the scaffolds.[27]

Table 2a. Summary of Conditions Used for Whole-Organ Scaffold Recellularization

Organ	*Authors*	*Cell population(s)*	*Cell numbers (million)*	*Seeding route (bolus injection/perfusion/other)*	*Perfusion flow rate/pressure*
Heart	Ott *et al.*, 2008	Rat cardiocytes	50–75	Intramural injection	6 mL/min
Lung	Ott *et al.*, 2010	Human carcinomatous alveolar cells	91.25 ± 31.72	Tracheal perfusion	10–15 mm Hg
Lung	Petersen *et al.*, 2010	Rat lung epithelial cells	100	Airway injection	1–5 mL/min
Lung	Cortiella *et al.*, 2010	Murine ESCs	2	Tracheal injection	(Nonperfusion)
Lung	Price *et al.*, 2010	Murine fetal lung cells	3	Infusion in culture medium	(Nonperfusion)
Lung	Song *et al.*, 2011	Rat fetal lung cells	Not stated	Tracheal perfusion	10–15 mm Hg
Liver	Uygun *et al.*, 2010	Rat hepatocytes	50	Bolus intravascular injection × 4	Not stated
Liver	Shupe *et al.*, 2010	Rat liver progenitor cells	1	Inferior vena caval injection	Not perfused or cultured
Liver	Soto-Gutierrez *et al.*, 2011	Murine hepatocytes	10–50	Intraparenchymal injection vs. steady perfusion vs. bolus injection	2 mL/min
Liver	Baptista *et al.*, 2011	Human fetal liver cells	70	Portal vein perfusion	3 mL/min
Liver	Barakat *et al.*, 2011	Human fetal stellate cells + human fetal hepatocytes	350 + 1000	Portal vein perfusion	90 mL/min
Kidney	Ross *et al.*, 2009	Murine ESCs	2	Arterial + ureteric injection	(Nonperfusion)
Liver, Kidney, Pancreas, Small bowel	Baptista *et al.*, 2009	Human HepG2 cells	30	Intravascular injection	6 mL/min

ESC, embryonic stem cell.

Table 2b. Summary of Recellularized Organ Construct Characterization and Techniques

Organ	*Authors*	*Histology/IF*	*TUNEL*	*EM*	*Functional assessment*	*In vivo implantation*
Heart	Ott *et al.*, 2008	+ / +	+	+	LV pressure monitoring + live video (contractility)	–
Lung	Ott *et al.*, 2010	+ / +	–	+	Dynamic lung fn tests, blood gases, live video	+
Lung	Petersen *et al.*, 2010	+ / +	+	+	Compliance testing, blood gases	+
Lung	Cortiella *et al.*, 2010	– / +	+	–	–	–
Lung	Price *et al.*, 2010	– / +	–	–	–	–
Liver	Uygun *et al.*, 2010	+ / +	+	+	LDH/urea/albumin assay RT-PCR of enzymes	+
Liver	Shupe *et al.*, 2010	+ / –	–	–	–	–
Liver	Soto-Gutierrez *et al.*, 2011	+ / +	–	–	Albumin/cytochrome/ammonia assay	–
Liver	Baptista *et al.*, 2011	+ / +	+	–	Urea/albumin/prostacylin assays Platelet deposition studies	–
Liver	Barakat *et al.*, 2011	+ / – (IHC)	+	–	Urea/albumin/lactate assays	+
Kidney	Ross *et al.*, 2009	+ / – (IHC)	–	–	–	–
Liver, Kidney, Pancreas, Small bowel	Baptista *et al.*, 2009	+ / – (IHC)	–	–	–	–

LV, left ventricle; LDH, lactate dehydrogenase; RT-PCR, reverse transcriptase–polymerase chain reaction.

Common trends seen within published protocols

The main parameters of interest for the perfusion decellularization and recellularization protocols are compared and summarized in Tables 1a–d and 2a and b, respectively.

Table 1a shows the different animal species and strains used, with the most common being rat, although there is an intentional move toward larger species to scale-up the technique to approach more human-sized organ constructs.

Table 1b displays the most common decellularizing agents used, with the predominance of SDS whether alone or in combination with Triton X-100. When another agent is quoted, there is a far wider disparity between protocols that almost vary from article to article (7 out of 18 in total). There are also other marked differences in protocols such as the additional use of physical methods (freezing) and whether DNAse or RNAse is also employed in combination with the main decellularizing agent (full details in Appendix Tables A1 and A2).

Table 1c summarizes the decellularization pump setup parameters, that is, flow rate (or pressure) and duration of decellularization (for the entire protocol, including periods of nonperfusion if relevant). While flow rates vary widely depending on the animal species, generally the rates adopted tend to be low and subphysiological vascular flow rates, while flow pressures tend to mimic physiological *in situ* ones. The total duration of the decellularization protocol gives an indication of how widely varying the protocols can be from group to group, whether in terms of the additional steps/methods used, for example, freezing, storage phases within the decellularization process, and the flow rates and concentrations applied with even the same decellularizing agents. The most marked contrast may be seen between De Kock *et al.* and Uygun *et al.* in work on the liver bioscaffold (1–2 h vs. up to 5 days), especially as the former quote directly from the latter as a baseline for developing their more streamlined protocol.

Table 1d summarizes the characterization of the decellularized organ scaffold and the techniques used; there is a common panel of tests to demonstrate a variety of important structural properties preserved in the ECM that are necessary for both the effectiveness of the bioscaffold for subsequent recellularization and the decellularization process itself. As can be seen, groups vary in how much of this panel of tests are completed. Not shown are any functional tests of ECM bioactivity, as this is limited so far to single growth factor assays and in two groups only.[23,25]

Table 2a summarizes the four main parameters in the recellularization protocols: cell population, cell numbers, route of seeding, and perfusion rate. The bioreactor conditions tend to be similar, that is, incubator conditions, and duration of continuous culture is on average 7 days (with one group moving onto a longer period[21]), and hence these parameters have been omitted from the table. Full details can be found in Appendix Table A2. Cell populations used have been commonly the mixed population-native cells isolated from fetal or neonatal organs as the initial proof of concept, but work is now moving onto human cell populations and stem cell populations to demonstrate biocompatibility and the bioinductive properties of the ECM scaffold. Cell numbers are by necessity high, for example, 50–100 million on rat-derived scaffolds, but exponentially higher on larger species; however, this is usually still only 10%–20% of normal physiological cell numbers. The route of seeding can depend on the physiological compartments available (other than the vascular), for example, the airway, and also direct injection is possible, but most researchers utilize the vascular route. There has been some comparison between a continuously perfused seeding process and a bolus intravascular injection, with some evidence that the latter affords higher engraftment.[17]

Table 2b displays those techniques for characterization of the recellularized organ constructs (where applicable), and these are usually a combination of histology-based techniques and functional testing specific to the organ/tissue in question.

Summary

In terms of decellularization protocols, these vary widely in many aspects, for example, strain/species of animal used, decellularization agents and other parameters (plus postdecellularization sterilization) to achieve the whole-organ ECM scaffold required for recellularization. On one hand, this is an indication of the universal applicability of the principle of perfusion decellularization to all animal tissues, and while variations in the optimal protocol can also be attributed to differences in the nature of each type of organ/tissue and its specific structure and composition, it also appears that a complete and systematic rationale for determining the optimal perfusion decellularization process has not yet been achieved. Some studies have started to formally assess achieved of decellularization protocols, for example, scaffold properties with varying number of decellularization cycles,[26] while only one study reports direct optimization from a baseline protocol taken from another study.[23] Characterization of the structural components of the ECM has yielded similar methods and results across most of the groups, but only two groups have attempted to assess the presence of the (presumed) bioinductive molecules present in the ECM with a quantification assay of two specific growth factors.[23,25] This is an area that requires further investigation in all the organs/tissues of relevance, as regulatory and standardization issues (e.g., quality control and release criteria) are fundamental to the clinical translation and commercialization of these ECM products. ECM products are known to vary from batch to batch (even animal to animal), and hence standardization of basic parameters (species/strain, gender, age, and weight) needs to be maintained to achieve meaningful comparison in outcomes, or from group to group. These donor factors, and others relating to the use of biological agents within certain protocols, may require a degree of dynamicity within the decellularization process, but currently the extreme disparity between some protocols suggests the need for a more evidence-based approach. Preoptimization and standard operating procedures are even more critical when it is likely that postprocessing testing of the ECM bioscaffold (and the recellularized construct) is likely to be limited in scope in those cases destined for implantation. Minimum standardized biological requirements within whole-organ ECM scaffolds (e.g., threshold DNA levels and structural integrity growth factor levels/activity) should also be established to maintain biological quality and clinical safety.

Regarding the recellularization process, most groups use a similar anatomical approach to the vascular perfusion setup for circulation of medium during continuous culture and

also use appropriate physiological adjuncts to help stimulate constructive remodeling (e.g., in the heart and lung models). Most groups have investigated the use of a mixed population of organ-specific cells isolated from neonatal or fetal animals to seed the acellular ECM scaffold as proof of concept and also to achieve the full extent of cellular variety and density required to populate a whole-organ scaffold. Several groups have also attempted reseeding with embryonic stem cells, which have demonstrated proliferation and differentiation specific to organ-specific bioinductive cues within the ECM scaffold. In addition, human cell populations have also been seeded onto the xenogeneic scaffolds to demonstrate biocompatibility. Again, there are quite widely varying parameters for the recellularization protocol between groups in terms of cell numbers and culture conditions, and this is an area where further systematic optimization is required. A physiological degree of cellular engraftment has not yet been achieved with any group, partly because of the very large cell numbers required. Finally, functional assessment of recellularized constructs depends on the degree of recellularization achieved and varies from organ to organ and whether the graft is suitable for implantation *in vivo*. Generally, only very short-term viability and implantation *in vivo* have been achieved so far (e.g., 6 h), but one study has expanded this into a 7-day implantation period after improving graft preservation.[21]

Appendix Tables A1 and A2 summarize further details of the decellularization and recellularization protocols used in the work published from the groups above.

Future Work and Considerations: Surgical Implantation of Bioartificial Organ Constructs

It has been shown so far that whole-organ decellularization can yield whole-organ ECM bioscaffolds capable of supporting recellularization on a complex 3D level and sustaining appropriate cellular and tissue functionality. These bioartificial organ constructs also allow relatively easy surgical manipulation, especially as they preserve the intact vascular pedicle for direct anastomosis at the orthotopic implantation site. The intact and inherent vasculature permits direct perfusion of the tissue and maintains provision of nutrients and oxygen to the implanted graft, in an exact parallel to the transplant procedure. As such, this technique could provide an ideal shortcut to bioengineering an organ replacement that is structurally and histologically similar to the original organ in question, uses established surgical procedures for implantation, is able to potentially support cellular function to the same degree, is biologically compatible, and comes from a widely available source (e.g., porcine or other xenogeneic organs).[7]

Currently, there are limitations to all the tissue-engineered organ constructs produced so far in terms of functionality and viability *in vivo*, varying from achieving sufficient or comparable to normal cellular density, achieving full cellular and tissue differentiation, and assessment of long-term viability, functionality, and constructive remodeling of organ grafts implanted *in vivo*. It would also be necessary to expand these techniques on larger-animal organs, which are closer in size and functionality to human ones. These are issues to be addressed and optimized before work can proceed to the clinical stage, in conjunction with the regulatory issues that guide cell choice (such as those as by the U.S. Food and Drug Administration regarding the use of autologous human cells applied in a nonhomologous location, or the use of allogeneic cells in virtually all cases), as well as a common language for reporting outcomes in trials.

In addition, it would be important to investigate the possibility of organ regeneration from an alternative cell source such as a stem cell population. Possibilities for this may be embryonic stem cells as has been tried in the lung or mesenchymal stem cells, which can differentiate into functional nephrons after injection into the nephrogenic site of developing rat embryos,[84] and are furthermore involved in the repair and recovery of renal function after acute renal injury.[85,86] If eventually autologous cells such as mesenchymal stem cells from the recipient alone could be used to create a functional organ graft, there could be significant clinical implications in overcoming the immune barrier and problem of rejection, with further great potential benefits to the patient.

Acknowledgments

With warm thanks to Prof Molly M Stevens for her advice and guidance with the text. In addition, M He is supported by the Royal College of Surgeons of England Research Fellowship program; A Callanan is supported by the Irish Research Council for Science, Engineering and Technology (IRCSET), and Marie Curie International Mobility Fellowship cofund grant (PD/2010/INSP/1948).

Disclosure Statement

No competing financial interests exist.

References

1. Bird, S.M., and Harris, J. Time to move to presumed consent for organ donation. BMJ **340,** 2188, 2010.
2. Place, E.S., Evans, N.D., and Stevens, M.M. Complexity in biomaterials for tissue engineering. Nat Mater **8,** 457, 2009.
3. Crapo, P.M., Gilbert, T.W., and Badylak, S.F. An overview of tissue and whole organ decellularization processes. Biomaterials **32,** 32, 2011.
4. Badylak, S.F. The extracellular matrix as a biologic scaffold material. Biomaterials **28,** 3587, 2007.
5. Badylak, S.F., Taylor, D., and Uygun, K. Whole-organ tissue engineering: decellularization and recellularization of three-dimensional matrix scaffolds. Annu Rev Biomed Eng **13,** 27, 2011.
6. Badylak, S.F., Weiss, D. J. Caplan, A., and Macchiarini, P. Engineered whole organs and complex tissues. Lancet **379,** 943, 2012.
7. Taylor, D.A. From stem cells and cadaveric matrix to engineered organs. Curr Opin Biotech **20,** 598, 2009.
8. Song, J.J., and Ott, H.C. Organ engineering based on decellularized matrix scaffolds. Trends Mol Med **17,** 424, 2011.
9. Gilbert, T.W. Strategies for tissue and organ decellularization. J Cell Biochem **113,** 2217, 2012.
10. Ott, H.C., *et al.* Perfusion-decellularized matrix: using nature's platform to engineer a bioartificial heart. Nat Med **14,** 213, 2008.
11. Ott, H.C., *et al.* Regeneration and orthotopic transplantation of a bioartificial lung. Nat Med **16,** 927, 2010.
12. Wainwright, J.M., *et al.* Preparation of cardiac extracellular matrix from an intact porcine heart. Tissue Eng Part C Methods **16,** 525, 2010.

13. Cortiella, J., *et al.* Influence of acellular natural lung matrix on murine embryonic stem cell differentiation and tissue formation. Tissue Eng Part A **16,** 2565, 2010.
14. Petersen, T.H., *et al.* Tissue-engineered lungs for in vivo implantation. Science **329,** 538, 2010.
15. Price, A.P., *et al.* Development of a decellularized lung bioreactor system for bioengineering the lung: the matrix reloaded. Tissue Eng Part A **16,** 2581, 2010.
16. Shupe, T., *et al.* Method for the decellularization of intact rat liver. Organogenesis **6,** 134, 2010.
17. Uygun, B.E., *et al.* Organ reengineering through development of transplantable recellularized liver graft using decellularized liver matrix. Nat Med **16,** 814, 2010.
18. Baptista, P.M., *et al.* Whole organ decellularization - a tool for bioscaffold fabrication and organ bioengineering. Conf Proc IEEE Eng Med Biol Soc **2009,** 6526, 2009.
19. Liu, C.X., *et al.* [Preparation of whole-kidney acellular matrix in rats by perfusion]. Nan Fang Yi Ke Da Xue Xue Bao **29,** 979, 2009.
20. Ross, E.A., *et al.* Embryonic stem cells proliferate and differentiate when seeded into kidney scaffolds. J Am Soc Nephrol **20,** 2338, 2009.
21. Song, J.J., Kim, S.S., Liu, Z., Madsen, J.C., Mathisen, D.J., Vacanti, J.P., and Ott, H.C. Enhanced in vivo function of bioartificial lungs in rats. Ann Thorac Surg **92**, 998, 2011.
22. Baptista, P.M., Siddiqui, M.M., Lozier, G., Rodriguez, S.R., Atala, A., and Soker, S., The use of whole organ decellularization for the generation of a whole liver organoid. Hepatology **53**, 604, 2011.
23. De Kock, J., Ceelen, L., De Spiegelaere, W., Casteleyn, C., Claes, P., Vanhaecke, T., and Rogiers, V. Simple and quick method for whole-liver decellularization: a novel in vitro three-dimensional bio-engineering tool? Arch Toxicol **85**, 607, 2011.
24. Barakat, O., Abbasi, S., Rodriguez, G., Rios, J., Wood, R.P., Ozaki, C., Holley, L.S., and Gauthier, P.K. Use of decellularized porcine liver for engineering humanized liver organ. J Surg Res **173**, e11, 2012.
25. Soto-Gutierrez, A., Zhang, L., Medberry, C., Fukumitsu, K., Faulk, D., Jiang, H., Reing, J., Gramignoli, R., Komori, J., Ross, M., Nagaya, M., Lagasse, E., Stolz, D., Strom, S.C., Fox, I.J., and Badylak, S.F. A whole organ regenerative medicine approach for liver replacement. Tissue Eng Part C Methods **17**, 677, 2011.
26. Totonelli, G., Maghsoudlou, P., Garriboli, M., Riegler, J., Orlando, G., Burns, A.J., Sebire, N.J., Smith, V.V., Fishman, J.M., Ghionzoli, M., Turmaine, M., Birchall, M.A., Atala, A., Soker, S., Lythgoe, M.F., Seifalian, A., Pierro, A., Eaton, S., and De Coppi, P. A rat decellularized small bowel scaffold that preserves villus crypt architecture for intestinal regeneration. Biomaterials **33**, 3401, 2012.
27. Perniconi, B., Costa, A., Aulino, P., Teodori, L., Adamo, S., and Coletti, D. The pro-myogenic environment provided by whole organ scale acellular scaffolds from skeletal muscle. Biomaterials **32**, 7870, 2011.
28. Gilbert, T.W., *et al.* Collagen fiber alignment and biaxial mechanical behavior of porcine urinary bladder derived extracellular matrix. Biomaterials **29,** 4775, 2008.
29. Sacks, M.S., and Gloeckner, D.C. Quantification of the fiber architecture and biaxial mechanical behavior of porcine intestinal submucosa. J Biomed Mater Res **46,** 1, 1999.
30. Brown, B., *et al.* The basement membrane component of biologic scaffolds derived from extracellular matrix. Tissue Eng **12,** 519, 2006.
31. Bissell, M.J., and Aggeler, J. Dynamic reciprocity: how do extracellular matrix and hormones direct gene expression? Prog Clin Biol Res **249,** 251, 1987.
32. Kleinman, H.K., Philp, D., and Hoffman, M.P. Role of the extracellular matrix in morphogenesis. Curr Opin Biotechnol **14,** 526, 2003.
33. Rosso, F., *et al.* From cell-ECM interactions to tissue engineering. J Cell Physiol **199,** 174, 2004.
34. Gilbert, T.W., *et al.* Degradation and remodeling of small intestinal submucosa in canine Achilles tendon repair. J Bone Joint Surg Am **89,** 621, 2007.
35. Badylak, S., *et al.* Resorbable bioscaffold for esophageal repair in a dog model. J Pediatr Surg **35,** 1097, 2000.
36. Ritchey, M.L., and Ribbeck, M. Successful use of tunica vaginalis grafts for treatment of severe penile chordee in children. J Urol **170(4 Pt 2),** 1574, discussion 1576, 2003.
37. Badylak, S.F., *et al.* The use of xenogeneic small intestinal submucosa as a biomaterial for Achilles tendon repair in a dog model. J Biomed Mater Res **29,** 977, 1995.
38. Boruch, A.V., *et al.* Constructive remodeling of biologic scaffolds is dependent on early exposure to physiologic bladder filling in a canine partial cystectomy model. J Surg Res **161,** 217, 2010.
39. Badylak, S.F., *et al.* Biologic scaffolds for constructive tissue remodeling. Biomaterials **32,** 316, 2011.
40. Hodde, J.P., *et al.* Vascular endothelial growth factor in porcine derived extracellular matrix. Endothelium **8,** 11, 2001.
41. Hodde, J.P., Ernst, D.M., and Hiles, M.C. An investigation of the long-term bioactivity of endogenous growth factor in OASIS Wound Matrix. J Wound Care **14,** 23, 2005.
42. Voytik-Harbin, S.L., *et al.* Identification of extractable growth factors from small intestinal submucosa. J Cell Biochem **67,** 478, 1997.
43. McDevitt, C.A., Wildey, G.M., and Cutrone, R.M. Transforming growth factor-beta1 in a sterilized tissue derived from the pig small intestine submucosa. J Biomed Mater Res A **67,** 637, 2003.
44. Hodde, J.P., *et al.* Retention of endothelial cell adherence to porcine-derived extracellular matrix after disinfection and sterilization. Tissue Eng **8,** 225, 2002.
45. Hodde, J., *et al.* Fibronectin peptides mediate HMEC adhesion to porcine-derived extracellular matrix. Biomaterials **23,** 1841, 2002.
46. Badylak, S.F., *et al.* Marrow-derived cells populate scaffolds composed of xenogeneic extracellular matrix. Exp Hematol **29,** 1310, 2001.
47. Zantop, T., *et al.* Extracellular matrix scaffolds are repopulated by bone marrow-derived cells in a mouse model of achilles tendon reconstruction. J Orthop Res **24,** 1299, 2006.
48. Badylak, S.F., *et al.* Comparison of the resistance to infection of intestinal submucosa arterial autografts versus polytetrafluoroethylene arterial prostheses in a dog model. J Vasc Surg **19,** 465, 1994.
49. Badylak, S.F., *et al.* Host protection against deliberate bacterial contamination of an extracellular matrix bioscaffold versus Dacron mesh in a dog model of orthopedic soft tissue repair. J Biomed Mater Res B Appl Biomater **67,** 648, 2003.
50. Brennan, E.P., *et al.* Antibacterial activity within degradation products of biological scaffolds composed of extracellular matrix. Tissue Eng **12,** 2949, 2006.
51. Medberry, C.J., *et al.* Resistance to Infection of Five Different Materials in a Rat Body Wall Model. J Surg Res **173,** 38, 2012.
52. Sarikaya, A., *et al.* Antimicrobial activity associated with extracellular matrices. Tissue Eng, **8**(1), 63, 2002.

53. Malmsten, M., Davoudi, M., and Schmidtchen, A. Bacterial killing by heparin-binding peptides from PRELP and thrombospondin. Matrix Biol **25,** 294, 2006.
54. Li, F., *et al.*, Low-molecular-weight peptides derived from extracellular matrix as chemoattractants for primary endothelial cells. Endothelium **11,** 199, 2004.
55. Orberg, J., Baer, E., and Hiltner, A. Organization of collagen fibers in the intestine. Connect Tissue Res **11,** 285, 1983.
56. Orberg, J.W., Klein, L., and Hiltner, A. Scanning electron microscopy of collagen fibers in intestine. Connect Tissue Res **9,** 187, 1982.
57. Badylak, S.F., Freytes, D.O., and Gilbert, T.W. Extracellular matrix as a biological scaffold material: Structure and function. Acta Biomaterialia **5,** 1, 2009.
58. Record, R.D., *et al.* In vivo degradation of 14C-labeled small intestinal submucosa (SIS) when used for urinary bladder repair. Biomaterials **22,** 2653, 2001.
59. Gilbert, T.W., Stewart-Akers, A.M., and Badylak, S.F. A quantitative method for evaluating the degradation of biologic scaffold materials. Biomaterials **28,** 147, 2007.
60. Martinod, E., *et al.* Tracheal regeneration following tracheal replacement with an allogenic aorta. Ann Thorac Surg **79,** 942, 2005.
61. Makris, D., *et al.* Tracheal replacement with cryopreserved allogenic aorta. Chest **137,** 60, 2010.
62. McPherson, T.B., *et al.* Galalpha(1,3)Gal epitope in porcine small intestinal submucosa. Tissue Eng **6,** 233, 2000.
63. Raeder, R.H., *et al.* Natural anti-galactose alpha1,3 galactose antibodies delay, but do not prevent the acceptance of extracellular matrix xenografts. Transpl Immunol **10,** 15, 2002.
64. Zhai, Y., Ghobrial, R.M., and Kupiec-Weglinski, J.W. Th1 and Th2 cytokines in organ transplantation: paradigm lost? Crit Rev Immunol **19,** 155, 1999.
65. Chen, N., Gao, Q., and Field, E.H. Prevention of Th1 response is critical for tolerance. Transplantation **61,** 1076, 1996.
66. Bach, F.H., *et al.* Accomodation of vascularised xenografts: expression of "protective genes" by donor endothelial cells in a host Th2 cytokine environment. Nat Med **3,** 196, 1997.
67. Piccotti, J.R., *et al.* Are Th2 helper T lymphocytes beneficial, deleterious or irrelevant in promoting allograft survival? Transplantation **63,** 619, 1997.
68. Allman A.J., *et al.* Xenogeneic extracellular matrix grafts elicit a TH2-restricted immune response. Transplantation **71,** 1631, 2001.
69. Allman, A.J., *et al.* The Th2-restricted immune response to xenogeneic small intestinal submucosa does not influence systemic protective immunity to viral and bacterial pathogens. Tissue Eng **8,** 53, 2002.
70. Brown, B.N., *et al.* Macrophage polarization: an opportunity for improved outcomes in biomaterials and regenerative medicine. Biomaterials **33,** 3792, 2012.
71. Badylak, S.F., *et al.* Macrophage phenotype as a determinant of biologic scaffold remodeling. Tissue Eng Part A **14,** 1835, 2008.
72. Brown B.N. *et al.* Macrophage phenotype as a predictor of constructive remodeling following the implantation of biologically derived surgical mesh materials. Acta Biomater **8,** 978, 2011.
73. Valentin, J.E., *et al.* Macrophage participation in the degradation and remodeling of extracellular matrix scaffolds. Tissue Eng Part A **15,** 1687, 2009.
74. Nagata, S., Hanayama, R., and Kawane, K. Autoimmunity and the clearance of dead cells. Cell **140,** 619, 2010.
75. Brown, B.N., *et al.* Macrophage phenotype and remodelling outcomes in response to biologic scaffolds with and without a cellular component. Biomaterials **30,** 1482, 2009.
76. Zhang, Q., *et al.* Circulating mitochondrial DAMPs cause inflammatory responses to injury. Nature **464,** 104, 2010.
77. Zheng, M.H., *et al.* Porcine small intestine submucosa (SIS) is not an acellular collagenous matrix and contains porcine DNA: possible implications in human implantation. J Biomed Mater Res B Appl Biomater **73,** 61, 2005.
78. Gorschewsky, O. *et al.* Quantitative analysis of biochemical characteristics of bone-patellar tendon-bone allografts. Biomed Mater Eng **15,** 403, 2005.
79. Rosario, D.J., *et al.* Decellularization and sterilization of porcine urinary bladder matrix for tissue engineering in the lower urinary tract. Regen Med **3,** 145, 2008.
80. Freytes, D.O., Stoner, R.M., and Badylak, S.F. Uniaxial and biaxial properties of sterilized porcine urinary bladder matrix scaffolds. J Biomed Mater Res B Appl Biomater **84,** 408, 2008.
81. Sun W.Q., and Leung, P. Calorimetric study of extracellular tissue matrix degradation and instability after gamma irradiation. Acta Biomater **4,** 817, 2008.
82. Qiu, Q.Q. *et al.* Inactivation of bacterial spores and viruses in biological material using supercritical carbon dioxide with sterilant. J Biomed Mater Res B Appl Biomater **91,** 572, 2009.
83. Nakayama, K.H., *et al.* Decellularized rhesus monkey kidney as a three-dimensional scaffold for renal tissue engineering. Tissue Eng Part A **16,** 2207, 2010.
84. Yokoo, T., *et al.* Human mesenchymal stem cells in rodent whole embryo culture are reprogrammed to contribute to kidney tissues. Proc Natl Acad Sci U S A **102,** 3296, 2005.
85. Morigi, M., *et al.* Life-sparing effect of human cord blood mesenchymal stem cells in experimental acute kidney injury. Stem Cells **28,** 513, 2010.
86. Morigi, M., *et al.* Mesenchymal stem cells are renotropic, helping to repair the kidney and improve function in acute renal failure. J Am Soc Nephrol **15,** 1794, 2004.

Address correspondence to:
Ming He, MBBS
Department of Bioengineering and Materials
Institute of Biomedical Engineering
Imperial College London
London SW7 2AZ
United Kingdom

E-mail: m.he10@imperial.ac.uk

Received: June 8, 2012
Accepted: October 17, 2012
Online Publication Date: December 14, 2012

(Appendix follows →)

Appendix Table A1. Summary of the Decellularization Protocols Used in the Literature

			Decellularization protocol				
Organ	*Authors*	*Tissue harvesting (species/strain/age, explantation details)*	*Perfusion type*	*Agent(s) + duration*	*Flow rate/pressure*	*Sterilization*	*Characterization of decellularised scaffold*
Heart	Ott *et al.*, 2008	12-week-old Fischer 344 rats Systemic heparinization	Retrograde coronary perfusion via ascending aorta	Heparinized PBS + 10 μM adenosine for 15 mins + 1% SDS for 12 h + 1% Triton X-100 for 30 mins	77.4 mm Hg coronary arterial pressure	PBS + 100 μ/mL pen-strep for 124 h	Histology + immunofluorescence of ECM–collagen I + III, laminin, fibronectin Aortic valve–Evans blue perfusion SEM/TEM of ECM architecture Vascular corrosion resin casting + heterotopic transplantation Mechanical (stress-strain/ tangential modulus) testing
Heart	Wainwright *et al.*, 2010	Adult pigs (strain not specified)	Retrograde coronary perfusion via ascending aorta	Frozen at −80°C for 16 h then thawed at room temperature (RT) + hypotonic type 1 water for 15 mins + 0.02% trypsin/0.05% EDTA/0.05% NaN3 for 2 h + 3% Triton X-100/0.05% EDTA/0.05% NaN3 for 2 h + 4% deoxycholic acid for 2 h	1–1.3 L/min	0.1% peracetic acid/4% ethanol for 4 h at 1.7 L/min	Histology + IHC/ immunofluorescence of ECM–DAPI, elastin, collagens (I, III, IV), GAGs DNA/GAG/elastin quantitative assays SEM of ECM architecture Mechanical (ball burst) testing
Lung	Ott *et al.*, 2010	12-week-old male Sprague-Dawley rats Systemic heparinization	Retrograde pulmonary arterial perfusion	Heparinized PBS for 15 mins + 0.1% SDS for 120 mins + 1% Triton-X100 for 10 mins	30 mm Hg pulmonary arterial pressure	PBS + 100u/mL pen-strep for 72 h	Histology of ECM–collagen, proteoglycans, elastin + Morphometry and stereology of alveoli TEM of ECM alveolar architecture Dynamic lung testing–compliance + vital capacity
Lung	Petersen *et al.*, 2010	3-month-old Fischer 344 rats Intraperitoneal heparin	Antegrade perfusion via right ventricle	PBS + 50 μ/mL + 1 μg/mL SNP + 8 mM CHAPS/1M NaCl/25 mM EDTA in PBS until total 500 mL of fluid perfused + 90 μ/mL benzonase	<20 mm Hg pulmonary arterial pressure	PBS + 10% pen-strep (duration not stated)	Histology + immunofluorescence of ECM–elastin, collagen I + IV, laminin, fibronectin DNA/collagen/GAG/elastin quantitative assays SEM/TEM of ECM architecture Micro-CT of vascular + alveolar architecture Mechanical (stress–strain/ compliance) testing
Lung	Cortiella *et al.*, 2010	Rats (age/strain not specified)	Mechanical agitation within bioreactor + initial freezing process	Frozen at −70°C for then thawed at 40°C /flash frozen×4 times + 1% SDS with continuous circulation for 5 weeks + DNAse/RNAse	(2.5 rpm rotational speed within bioreactor)	PBS + pen-strep + amphotericin for 24 h	Immunofluorescence—DAPI, MHC-1 Gel electrophoresis of DNA content
Lung	Price *et al.*, 2010	2–3-month-old C57BL/6 female mice	Injection via right ventricle + trachea	0.1% Triton X-100 2% sodium deoxycholate DNase Repeated injection/incubation steps—not continuous perfusion	N/A	All solutions sterile with added pen-strep	Histology + immunofluorescence of ECM–collagen, elastin, DAPI, laminin Collagen/GAG/laminin/elastin quantitative assays SEM of ECM architecture Pulmonary function tests
Lung	Song *et al.*, 2011	Male Sprague-Dawley rats (260–280 g) Systemic heparinization	Antegrade pulmonary arterial perfusion	Heparinized PBS for 15 mins + 0.1% SDS for 120 mins + 1% Triton-X100 for 10 mins	80 cm H_2O	PBS + 100u/mL pen-strep for 72 h	(Not performed)
Liver	Uygun *et al.*, 2010	Female adult (150–200 g) Lewis rats	Antegrade perfusion via portal vein	Initial 20 mL 0.9% saline then frozen at −80°C for 4 h then thawed at	1 mL/min	PBS + 0.1% peracetic acid for 3 h	Histology + immunofluorescence of ECM–collagen I + IV, laminin,

(*continued*)

Appendix Table A1. (Continued)

			Decellularization protocol				
Organ	*Authors*	*Tissue harvesting (species/strain/age, explantation details)*	*Perfusion type*	*Agent(s) + duration*	*Flow rate/pressure*	*Sterilization*	*Characterization of decellularised scaffold*
		Intracardiac heparin		4°C + PBS at 1 mL/min overnight + 0.01% SDS for 72 h + 0.1% SDS for 24 h + 1% SDS for 24 h + 1% Triton-X100 for 30 mins			fibronectin DNA/collagen/GAG quantitative assays SEM of ECM architecture Vascular corrosion resin casting
Liver	Shupe *et al.*, 2010	Adult Fischer 344 rats	Retrograde perfusion via inferior vena cava	Initial 100 mL PBS + 1%, 2%, 3% Triton X-100 in sequence until 300 mL each perfused + 0.1% SDS until 300 mL perfused	5 mL/min	300 mL PBS	Histology + immunofluorescence of ECM–collagen IV, laminin, DAPI
Liver	Soto-Gutierrez *et al.*, 2011	Male adult (250–300 g) Sprague-Dawley rats Systemic heparinization	Retrograde perfusion via inferior vena cava	Initial 5–10 mL PBS/heparin, and then frozen at −80°C for 24 h then thawed at RT + 0.02% trypsin/0.05% EGTA for 2 h + 3% Triton X-100/0.05% EGTA for 18–24 h	8 mL/min	2MRad gamma irradiation	Histology + immunohistochemistry (IHC) of ECM–collagen IV, laminin, fibronectin, DAPI Gel electrophoresis of DNA content SEM/TEM of ECM architecture Vascular corrosion resin casting
Liver	Baptista *et al.*, 2011	Ferret (age/strain/gender not specified)	Antegrade perfusion via portal vein	Initial dH_2O (40× volume of liver) + 1% Triton X-100/0.1% NH_4OH (50× volume of liver)	5 mL/min	Not stated	IHC + Western blotting—collagen I/III/IV, laminin, fibronectin DNA/collagen/GAG quantitative assays SEM of ECM architecture Fluoroscopy + confocal microscopy of vasculature
Liver	De Kock *et al.*, 2011	Male adult (250–300 g) Sprague-Dawley rats Systemic heparinization	Antegrade perfusion via portal vein	Initial Krebs-Henseleit buffer for 15 mins + 1% Triton X-100 for 30 mins + 1% SDS for 30 mins	30 mL/min	N/A	Histology + IHC of ECM–collagen I + IV, laminin, fibronectin, VEGF SEM of ECM architecture Vascular corrosion resin casting
Liver	Barakat *et al.*, 2011	Yorkshire swine (25–35 kg)	Antegrade perfusion via portal vein	Initial 6–10 L dH_2O + 20 L 0.25% SDS (store in 0.25% SDS for 48 h) + 40 L 0.5% SDS over 2–3 h + 20 L dH_2O + 10% formalin + 40 L PBS	80 mm Hg	10% formalin	Histology + IHC of ECM–collagen I + IV, laminin, fibronectin Vascular corrosion resin casting + fluoroscopy
Kidney	Ross *et al.*, 2009	Male adult (250–300 g) Sprague-Dawley rats Systemic heparinization	Antegrade perfusion via renal artery	Initially saline + SNP + 3% Triton-X100, DNAse + 3% Triton-X100 + 4% SDS (durations not stated)	100 mm Hg	Not stated	Histology + IHC of ECM–collagen IV, laminin SEM of ECM architecture
Kidney	Liu *et al.*, 2009	12-week (180–220 g) Wistar rats	Antegrade perfusion via renal artery	Initial PBS/heparin for 15 mins + 1%SDS for 12 h + 1% Triton-X100 for 30 mins	100 cm H_2O	PBS + pen-strep for 48 h	Histology + immunofluorescence of ECM–DAPI SEM of ECM architecture
Liver, Kidney, Pancreas, Small bowel	Baptista *et al.*, 2009	Ferret liver Pig kidney/pancreas/small bowel	Not stated	1% Triton X-100/0.1% Ammonium hydroxide for 24 h or until translucent	10–60 mL/min	Not stated	Histology Fluoroscopy of vasculature
Small bowel	Totonelli *et al.*, 2012	Adult (320–350 g) Sprague-Dawley rats	Antegrade perfusion via superior mesenteric artery	Detergent–enzymatic treatment (DET): Deionized water for 24 h + 0.4% sodium deoxycholate for 4 h + 2000 kU DNAse for 3 h (1–4 cycles)	0.6 mL/h	N/A	Histology + IHC of ECM–MHC-II, SMA, vimentin, MNF116 DNA/collagen/GAG quantitative assays SEM/TEM of ECM architecture Mechanical testing—stress/strain
Skeletal muscle	Perniconi *et al.*, 2012	Adult BALB/C mice	(Incubation/rotation method)	1% SDS for 24 or 48 h	(N/A)	PBS washes	Histology + immunofluorescence of ECM–actin, laminin, fibronectin

PBS, phosphate-buffered saline; ECM, extracellular matrix; SDS, sodium dodecyl sulfate; SNP, sodium nitroprusside; SEM, scanning electron microscopy; TEM, transmission electron microscopy; N/A, not applicable; GAG, glycosaminoglycan; VEGF, vascular endothelial growth factor.

Appendix Table A2. Summary of the Recellularization Protocols Used in the Literature

		Recellularization protocol			
Organ	*Authors*	*Bioreactor setup/special conditions (in addition to vascular perfusion)*	*Cell population/numbers + reseeding*	*Culture conditions*	*Characterization of organ construct and functionality*
Heart	Ott *et al.*, 2008	Cannulation of left atrium and ascending aorta–pulsatile distension of left ventricle + compliance loop attached to ascending aorta to reproduce physiological preload, after-load and intraventricular pressure. Coordinated electrical stimulation at 5–20 V via electrodes	50–75 million rat neonatal cardiocytes isolated and seeded via intramural injection + 2 million rat aortic endothelial cells via perfusion	Culture medium (CM) perfused at atrial flow rate (FR) 20 mL/min, coronary FR 6 mL/min 37°C 5% CO_2 incubator Duration of culture: 4–8 days	Histology (engraftment) + immunofluorescence—TUNEL, α-actin, MHC, vWF, connexin-43 TEM of ultra-architecture Perfusion with CMFDA to demonstrate endothelialization LV pressure monitoring + live video to demonstrate contractile activity
Heart	Wainwright *et al.*, 2010	(Nonperfusion culture system: lyophilized sheets of cardiac ECM used)	500000 cells/cm^2 white leghorn chicken embryonic cardiomyocytes isolated	37°C 5% CO_2 incubator Duration of culture: 4 days	Immunofluoresence—α-actinin + β-tubulin to identify cardiomyocytes
Lung	Ott *et al.*, 2010	Perfusion system through pulmonary artery, left atrium, and trachea; pulmonary vein drained to equilibration chamber Trachea connected to gas ventilation chamber. Alternating air and fluid (culture medium) perfusion	91.25 ± 31.72 million carcinomatous human alveolar basal epithelial cells by gravity perfusion through trachea + 66.57 ± 18.22 human umbilical cord venous endothelial cells (HUVECs) by gravity perfusion of pulmonary artery and vein; 308.57 ± 146.9 million rat fetal lung cells isolated + HUVECs seeded via same method	CM perfused at 10–15 mm Hg constant pressure with negative pressure ventilation 37°C 5% CO_2 incubator Duration of culture: 5–9 days	Histology (engraftment) + immunofluorescence—caveolin-1, T1α, Ttf1, vimentin, pro-SPC TEM of ultra-architecture Immunoblotting–SP-A, SP-C Morphometry + stereology of lung architecture *In vitro* function testing–blood gas values, dynamic lung function tests Orthotopic transplantation into syngeneic male rats–fluoroscopy and live video, blood gas values
Lung	Petersen *et al.*, 2010	Pulmonary artery cannulation for perfusion loop Breathing loop/negative pressure ventilation via trachea cannulation + syringe pump	100 million rat neonatal lung epithelial cells isolated and injected into airway compartment + 30 million lung vascular endothelial cells via artery	CM perfused at 1–5 mL/min with negative pressure ventilation at 1 breath/min 37°C 5% CO_2 incubator Duration of culture: 4–8 days	Histology (engraftment, TUNEL) + immunofluorescence—CD-31, CCSP, pro-SPC, aquaporin-5, α-actin, Cy-14. TEM of ultra-architecture Stress-strain + compliance testing Orthotopic transplantation into syngeneic male Fischer 344 rats + blood gas values tested to demonstrate gas exchange
Lung	Cortiella *et al.*, 2010	(Nonperfusion bioreactor: rotating chamber system)	2 million murine embryonic stem cells (ESCs) injected into trachea (I million cells into each side/lung scaffold)	CM circulated by pump action at speed of 2 rpm 37°C 5% CO_2 incubator Duration of culture: 14–21 days	Immunofluorescence—DAPI, live/dead staining, TUNEL, cytokeratin 18, CD31, pro-SPC, laminin, collagen IV
Lung	Price *et al.*, 2010	(Nonperfusion bioreactor: scaffolds suspended in CM flasks) Tracheal cannulation for ventilation loop	3 million fetal lung cells isolated from day E17 gestation B6 mice infused into CM	Mechanical ventilation at 180 breaths/min (300 μL volume) 37°C 5% CO_2 incubator Duration of culture: 7 days	Immunofluorescence—DAPI, cytokeratin 18, CD31, pro-SPC, aquaporin-5, CCSP, CD45, CD11b, vimentin
Lung	Song *et al.*, 2011	Perfusion system through pulmonary artery, left atrium, and trachea; pulmonary vein drained to equilibration chamber Trachea connected to gas ventilation chamber Alternating air and fluid (culture medium) perfusion	Rat fetal lung cells + HUVECs (numbers not stated)	CM perfused at 1–5 mL/min with negative pressure ventilation at 1 breath/min 37°C 5% CO_2 incubator Duration of culture: 7–10 days	Histology + IHC–TTF-1, pro-SPC, CC10, CD31, vimentin Morphometry + stereology of lung architecture *In vitro* function testing—blood gas values, dynamic lung function tests Orthotopic transplantation into syngeneic male rats up to 14 days–fluoroscopy and live video, blood gas values
Liver	Uygun *et al.*, 2010	Portal vein cannulation for perfusion loop	50 million rat hepatocytes isolated and seeded via bolus intravascular injection×4 + 40 million cardiac endothelial cells via perfusion	Perfusion FR not stated 37°C 5% CO_2 incubator Duration of culture: 1–5 days	Histology (engraftment) + immunofluorescence—TUNEL, albumin, G6pc, Ugt1a LDH release quantification Urea + albumin synthesis quantification RT-PCR of drug metabolism enzymes Heterotopic transplantation into syngeneic rats + fresh blood perfusion model to test viability and hepatocyte function

(*continued*)

Appendix Table A2. (Continued)

		Recellularization protocol			
Organ	*Authors*	*Bioreactor setup/special conditions (in addition to vascular perfusion)*	*Cell population/numbers + reseeding*	*Culture conditions*	*Characterization of organ construct and functionality*
Liver	Shupe *et al.*, 2010	Inferior vena cava (IVC) cannulation, but no continuous perfusion culture performed	1 million rat liver progenitor cells WB344 via IVC injection	-	Histology
Liver	Soto-Gutierrez *et al.*, 2011	Portal vein cannulation for perfusion loop	10–50 million murine adult hepatocytes injected directly into parenchyma vs. perfusion in CM at 2 mL/min vs. perfused in multiple boluses	Perfusion FR 2 mL/min 37°C 5% CO_2 incubator Duration of culture: 7 days	Histology (engraftment) + immunofluorescence—DAPI, albumin, Ki67 Albumin synthesis/cytochrome activity/ ammonia metabolism quantification assays
Liver	Baptista *et al.*, 2011	Portal vein cannulation for perfusion loop	70 million human fetal liver cells + 30 million HUVECs coinfusion via portal vein	Perfusion FR 3 mL/min for seeding × 16 h; Perfusion FR 0.5 mL/min 37°C 5% CO_2 incubator Duration of culture: 7 days	Histology + immunofluorescence—TUNEL, Ki-67 Urea/albumin/prostacylin synthesis quantification Platelet deposition studies
Liver	De Kock *et al.*, 2011	N/A	N/A	N/A	N/A
Liver	Barakat *et al.*, 2011	Posterior segments only (x3) Portal vein cannulation for perfusion loop	350 million human fetal stellate cells + 1 billion human fetal hepatocytes via portal vein	Perfusion FR 90 mL/min 37°C 5% CO_2 incubator Duration of culture: 3–13 days	Histology + IHC–CK-18, CK-19, AFP, CYP3A4, TUNEL, Ki-67 Urea/albumin/lactate synthesis quantification Orthotopic transplantation - histology
Kidney	Ross *et al.*, 2009	Renal artery cannulation for perfusion loop, also cannulation of ureter	2 million murine pluripotent ES cells injected via artery or ureter	Sections of seeded graft cultured for 3–10 days 37°C 5% CO_2 incubator Perfusion of whole organ at 120/80 mm Hg for 6–10 days	Histology (engraftment + morphology) + IHC—pancytokeratin, Pax-2, Ksp-cadherin, KI-67 RT-PCR of Pax-2 + Ksp-cadherin expression
Kidney	Liu *et al.*, 2009	(N/A)	(N/A)	(N/A)	(N/A)
Liver, Kidney, Pancreas, Small bowel	Baptista *et al.*, 2009	Recellularization performed on ferret liver via portal vein cannulation and perfusion	30 million human HepG2 cells + 30 million mouse endothelial cells injected intravascularly	Perfusion FR 6 mL/min 37°C 5% CO_2 incubator Duration of culture: 7 days	Histology IHC–albumin, vWF, KI-67
Small bowel	Totonelli *et al.*, 2012	N/A	N/A	N/A	N/A
Skeletal muscle	Perniconi *et al.*, 2012	N/A	N/A	N/A	N/A

RT-PCR, reverse transcriptase–polymerase chain reaction; LDH, lactate dehydrogenase.